



An electrochemical and theoretical evaluation of new benzothiazine derivatives as a corrosion inhibitor for mild steel in HCl solutions

Nada Kheira Sebbar¹, Hicham Elmsellem^{2*}, Maria Boudalia³, Sanae lahmidi¹, Abdelkebir Belleaouchou³, Abdelah Guenbour³, El Mokhtar Essassi¹, Hanae Steli⁴, Abdelouahed Aouniti²

¹Laboratoire de Chimie Organique Heterocyclique, URAC 21, Pôle de Compétences Pharmacochimie, Université Mohammed V, Faculté des Sciences, Av. Ibn Battouta, BP 1014 Rabat, Morocco.

²Laboratoire de Chimie Appliquée et environnement (LCAE-URAC18), Faculté des Sciences, Université Mohammed Premier, Oujda, Morocco.

³Laboratory of Materials, Nanotechnology and Environment, Faculty of Science, University of Mohamed-V- Av. Ibn Battouta, BP 1014 Agdal-Rabat, Morocco.

⁴Laboratoire mécanique & énergétique, Faculté des Sciences, Université Mohammed Premier, Oujda, Morocco.

Received 1 Aug 2015; Revised Sept 16 2015; Accepted 16 Sept 2015.

*Corresponding Author. E-mail: h.elmsellem@yahoo.fr

Abstract

The inhibition effect of benzothiazine (3,4-dihydro-2H-1,4-benzothiazine-3-thione) : P₁ in mild steel corrosion in 1M HCL acid was investigated by weight loss, potentiodynamic polarization and electrochemical impedance spectroscopy (EIS) techniques. The result showed that corrosion rate was significantly decreased in presence of the inhibitor. The inhibiting action increases with the concentration of benzothiazine compound to attain 92 % at 10⁻³ mol/L. The increase in temperature leads to a decrease in the inhibition efficiency of the compounds in the temperature range 313-343K. Adsorption of benzothiazine P₁ on the mild steel surface in 1M HCL solution obeyed the Langmuir adsorption isotherm. Attempt to correlate the molecular structure to quantum chemical indices was made using density functional theory (DFT). EIS measurements showed an increase in charge transfer resistance (R_{ct}) with concentration. Potentiodynamic polarization study showed that the inhibitor act as mixed type, controlling both the anodic and cathodic reactions.

Keywords: Benzothiazine, mild steel, Corrosion, inhibition efficiency, EIS.

Introduction

In recent years, there has been an upsurge in the synthesis of non-steroidal anti-inflammatory drugs (NSAIDs) with two or more heterocyclic to overcome the drawbacks of known non-steroidal anti-inflammatory drugs (NSAIDs) such as aspirin, ibuprofen and naproxen. The search for novel analgesic and anti-inflammatory agents devoid of side effects continues to be an active area of research in medicinal chemistry. A number of 2H-1,4-benzothiazine derivatives were reported for their biological activities such as antimicrobial [1], antimalarial [2], anti-inflammatory [3], antifungal [4] and 15-lipoxygenase inhibition properties [5]. Have been reported as effective corrosion inhibitors for steel in acidic media. The heterocyclic compounds with functional groups containing hetero-atoms, which can donate lone pair electrons are found to be particularly useful as inhibitors for metal corrosion [6-9]. Recently more study shows that the inhibitive effect is found to enhance several nitrogen containing organic compounds for carbon steel in acid solutions. Organic nitrogen compounds which usually employed for their rapid action in acidic solutions specify the corrosion behavior of iron and steel [10].

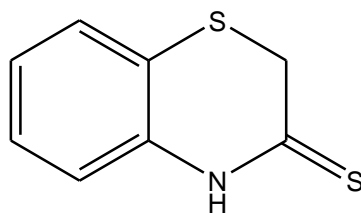
The objective of this investigation is to determine the corrosion inhibition efficiency of 3,4-dihydro-2H-1,4-benzothiazine-3-thione :P₁ as a novel inhibitor for the corrosion of mild steel in 1.0 M HCL. The inhibition efficiency was determined using two different techniques: electrochemical impedance spectroscopy (EIS) and potentiodynamic polarization measurements. Quantum chemical calculation was also employed to provide insight into the mechanism of the inhibitory action.

2. EXPERIMENTAL

2.1. Materials

Mild steel was used for this study has the following composition: Mild Steel strips containing (0.09 % P; 0.38 % Si; 0.01 % Al; 0.05 % Mn; 0.21 % C; 0.05 % S and the remainder iron.

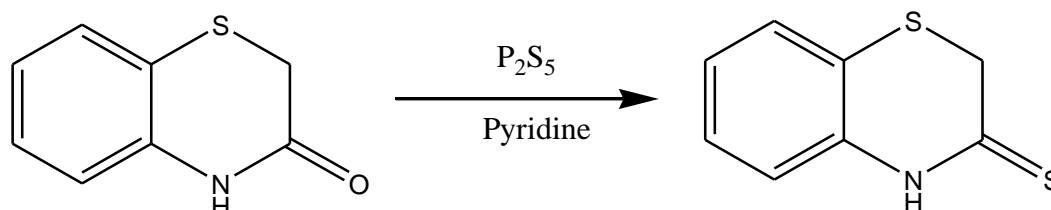
The specimen was used for electrochemical measurements. The exposed surface area was 1cm^2 .



Scheme.1: 2H-benzo[b][1,4]thiazine-3(4H)-thione

2.2. Synthesis of inhibitor

To a well-stirred solution of (5 g, 33.1mmol) 3,4-dihydro-2H-1,4-benzothiazine-3-one in 50 mL of dry pyridine was added (14.7g, 33.1mmol) phosphorus pentasulfide, the reaction mixture is heated to reflux for 4 hours, the solid obtained is washed several times with hot water, dried and then purified in absolute ethanol. Recrystallization is carried out in the petroleum ether. The product obtained was characterized by ^1H NMR, ^{13}C NMR.



Scheme 2: Characterization of 3,4-dihydro-2H-1,4-benzothiazine-3-thione : (P1)

Characterization of 3,4-dihydro-2H-1,4-benzothiazine-3-thione : (P1) Light yellow solid (75 % yield), mp: 126-128 °C. ^1H NMR (δ) 3.88 (s, 2H, $-\text{CH}_2-$), 7.02 (d, $J = 8.0$ Hz, 1H, aromatic), 7.10 (dd, $J = 7.8, 8.0$ Hz, 1H, aromatic), 7.20 (dd, $J = 7.8, 8.0$ Hz, 1H, aromatic), 7.34 (d, $J = 7.8$ Hz, 1H, aromatic), 10.40 (s, 1H, NH). ^{13}C NMR (δ) 37.5 (t), 117.9 (d), 122.9 (d), 125.7 (d), 127.5 (d), 128.4 (s), 136.1 (s), 192.5 (s).

2.3. Solutions

The aggressive solutions of 1.0 M HCl were prepared by dilution of an analytical grade 37% HCl with double distilled water. The concentration range of inhibitor employed was $10^{-5} - 10^{-3}$ (mol/l)

2.4. Weight loss method

Gravimetric measurements were carried out in a double-walled glass cell equipped with a thermostat cooling condenser. The solution volume was 50 mL. The steel specimens used had a rectangular form ($1.5\text{cm} \times 1.5\text{cm} \times 0.05\text{cm}$). The immersion time for the weight loss was 6 h at 308 K.

In order to get good reproducibility, experiments were carried out in duplicate. The average weight loss was obtained.

2. Electrochemical tests

2.1. Electrochemical impedance spectroscopy

The electrochemical measurements were carried out using Volta lab (Tacussel- Radiometer PGZ 301) potentiostat and controlled by Tacussel corrosion analysis software model (Volta master 4) at under static condition. The corrosion cell used had three electrodes. The reference electrode was a saturated calomel electrode (SCE). A platinum electrode was used as auxiliary electrode of surface area of 1cm^2 . The working electrode was mild steel. All potentials given in this study were referred to this reference electrode. The working electrode was immersed in test solution for $\frac{1}{2}$ hours to establish steady state open circuit potential (E_{ocp}). After measuring the E_{ocp} , the electrochemical measurements were performed. All electrochemical tests have been performed in aerated solutions at 308K. The EIS experiments were conducted in the frequency range with high limit of 100 KHz and different low limit 10 mHz at open circuit potential, with 10 points per decade, at the rest potential, after 30 min of acid immersion, by applying 10 mV ac voltage peak-to-peak.

Nyquist plots were made from these experiments and the impedance plots are given in the Nyquist representation. Experiments are repeated three times to ensure the reproducibility.

2.2. Potentiodynamic polarization

The electrochemical behavior of mild steel sample in inhibited and uninhibited solution was studied by recording anodic and cathodic potentiodynamic polarization curves. Measurements were performed in the 1.0 M HCL solution containing different concentrations of the tested inhibitor by changing the electrode potential automatically from -800 to -100 mV versus corrosion potential at a scan rate of 1 mV/s. The linear Tafel segments of anodic and cathodic curves were extrapolated to corrosion potential to obtain corrosion current densities (I_{corr}).

3. Results and Discussion

3.1. Potentiodynamic Polarization Curves

Figure 1. Shows the anodic and cathodic polarization curves for mild steel in 1M HCl at different concentrations of the benzothiazine derivatives (P_1) inhibitor.

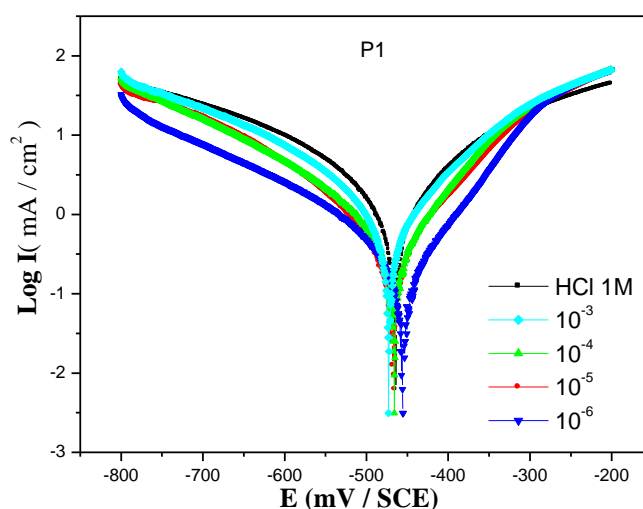


Figure 1. Potentiodynamic polarization curves of mild steel in 1M HCl in the presence of different concentrations of benzothiazine derivatives (P_1) at 308K

It's clear from this figure that the addition of the inhibitor concentration causes a significant decrease in the corrosion rate, a displacement of the anodic curves to more positive potentials and the cathodic curves to more negative potentials. This may be attributed to adsorption of the inhibitor on the electrode surface. Figure 1 shows the Tafel polarization curves for mild steel in 1.0 M Hydrochloric acid solution at different concentrations (10^{-3} to 10^{-6} M) of inhibitor at 308K. The inhibition efficiency values IE (%), were calculated using the following equation (1):

$$IE\% = \frac{I_{corr}^0 - I_{corr}}{I_{corr}^0} \quad (1)$$

Where I_{corr}^0 and I_{corr} are uninhibited and inhibited corrosion current densities, respectively. Values of the corrosion current densities (I_{corr}), corrosion potential (E_{corr}), cathodic Tafel slope (b_c), were calculated from Figure 1 and are listed in Table 1.

Data in Table 1 show that P_1 inhibit the corrosion process and the inhibition efficiency values ($\%IE$) increases with the concentration of inhibitor, reaching its maximum value is 93% at 10^{-3} M. These data show that the increase in inhibitor concentration leads to decrease in the corrosion current density. The presence of the P_1 concentration does not remarkable displacement of the corrosion potential, while the cathodic Tafel slope β_c change with the increase in the inhibitor concentration. These observations indicate that the P_1 inhibitor is a mixed-type inhibitor for the corrosion of mild steel in 1.0 M HCl [11]. This due to the adsorption of the inhibitor on the corroding surface [12, 13].

Table 1. Electrochemical parameters of mild steel in 1M HCl solution without and with benzothiazine derivatives (P₁) at different concentrations.

Inhibitor	Concentration (M)	-E _{corr} (mV/SCE)	I _{corr} (μA/cm ²)	-βc	βa	IE(%)
HCl 1M	-	464	1386	164	135	-
P ₁	10 ⁻³	456	102	82	68	93
	10 ⁻⁴	467	266	103	85	81
	10 ⁻⁵	466	320	110	80	77
	10 ⁻⁶	473	656	111	101	53

3.2. Electrochemical impedance spectroscopy

The impedance measurements were carried at 308 K after 30 min of immersion in 1M HCl solutions in the absence and presence of different concentrations of the P₁ inhibitor. The Nyquist plots for mild steel obtained at the interface in the presence and the absence of P₁ at different concentrations are given in figure 2.

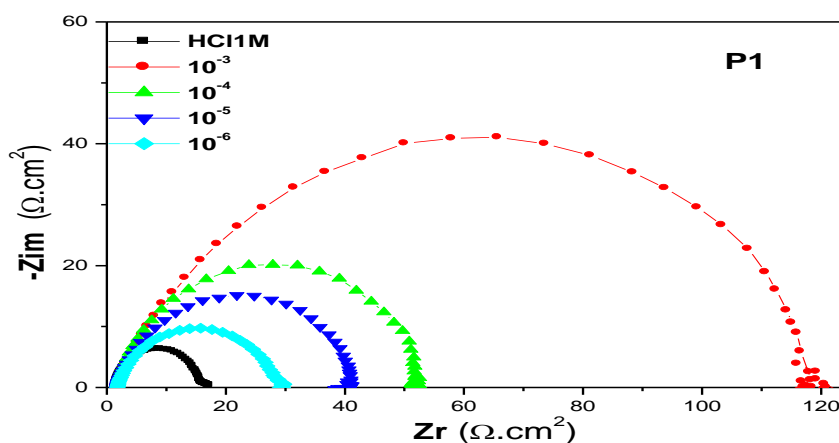


Figure 2. Nyquist plots for mild steel in 1 M HCl containing different concentrations of benzothiazine derivatives (P₁)

Figure 2 show the Nyquist plots present capacitive loops as a depressed semicircle, the diameter of the capacitive loop in the presence of inhibitor is larger than that in the absence of inhibitor and increases with the inhibitor concentration, indicating that the corrosion is primarily a charge transfer process and the formed inhibitive film increases by the addition of the inhibitor P₁ [14].

The charge-transfer resistance (R_{ct}) values are calculated from the difference in impedance at lower and higher frequencies as suggested by Tsuru et al [15]. The double layer capacitance (C_{dl}), the values of frequency at which the imaginary component of the impedance is maximum -Z_{im(max)} was found and used in the following equation (2) with corresponding R_{ct} values:

$$C_{dl} = \frac{1}{2\pi f_m R_t} \quad (2)$$

With C_{dl} Double layer capacitance (μF.cm⁻²); f_m: maximum Frequency (Hz) and R_t: Charge transfer resistance (Ω.cm²).

In this case, the inhibition efficiency is calculated using charge-transfer resistance from equation (3):

$$\%IE = \left(1 - \frac{R_{ct}^\circ}{R_{ct}}\right) \quad (3)$$

Where R_{ct}[°] and R_{ct} are the charge transfer resistance in the absence and presence of different concentrations of inhibitor, respectively.

Table 2. AC impedance data of mild steel in 1.0 M HCl acid solution containing different concentrations of P₁ at 308K.

Inhibitor	Concentration (M)	R _{ct} (Ω.cm ²)	C _{dl} (μf/cm ²)	IE (%)
HCl 1M	-	14.57	200	--
P ₁	10 ⁻³	118	68.04	88
	10 ⁻⁴	51	99.86	71
	10 ⁻⁵	41	99.49	64
	10 ⁻⁶	29	115.40	50

The experimental result of EIS measurements for the corrosion of mild steel in 1M HCl in the absence and presence of P₁ inhibitor is given in Table 2. As it can be observed from the table, the charge-transfer resistance values (R_{ct}) increased with increase in the concentration of the inhibitor, whereas the values of the capacitance of the interface (C_{dl}) starts decreasing with increase in inhibitor concentration, which is most probably due to the decrease in local dielectric constant and/or increase in thickness of the electrical double layer. This suggests that the inhibitor acts via adsorption at the metal/solution interface [16] and the decrease in the C_{dl} values is caused by the gradual replacement of water molecules by the adsorption of the inhibitor molecules on the electrode surface, which decreases the extent of metal dissolution [17]. The inhibiting effectiveness increases with the concentration of the inhibitor to reach a maximum value reach to a maximum value from 88% for P₁.

3.3. Weight Loss Measurements and adsorption isotherm

The effect of addition of P₁ compound tested at different concentrations on the corrosion of steel in 1.0 M HCl solution was studied by weight loss at 308K after 6h of immersion. The values of the percentage inhibition efficiency IE (%) were calculated from the following equation (4):

$$\%IE = \frac{W_{corr} - W'_{corr}}{W_{corr}} * 100 \quad (4)$$

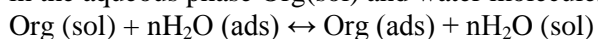
Where W_{corr} and W'_{corr} are weight loss in the absence and presence of inhibitor.

Table 3: Weight loss data of mild steel in 1 M HCl for various concentrations of the benzothiazine derivatives (P₁).

Inhibitor	Concentration (M)	Corrosion rate (mg cm ⁻² h ⁻¹)	IE (%)	θ
HCl 1M	—	0.820	—	—
P ₁	10 ⁻⁶	0.279	66	0.66
	10 ⁻⁵	0.141	83	0.83
	10 ⁻⁴	0.068	92	0.92
	10 ⁻³	0.031	96	0.96

Table 3 clearly indicates a decrease in the corrosion rate in the presence of all concentrations of this compound, P₁ inhibits the corrosion of mild steel and the efficiency inhibition increases with the increasing inhibitor concentration. This effect is hugely marked at higher concentration of inhibitor. The presence of inhibitor P₁ gave a high inhibiting. This is probably due to the presence of sulphur and nitrogen atom according to Every and Riggs [18]. The organic compound containing the nitrogen and sulphur has better inhibition efficiency in acidic media.

The adsorption process depends on the structural formula and electronic characteristics of the inhibitor, temperature, the nature of metal surface and the varying degrees of surface-site activity [19, 20]. In actual fact, the H₂O molecules could be adsorbed at the electrode /solution interface. To this effect, the adsorption of organic inhibitor molecules can be considered as a quasi substitution process between the organic compounds in the aqueous phase Org(sol) and water molecules at the electrode surface H₂O(ads) [21]:



Where (n) is the size ratio, that is the number of water molecules replaced by one organic inhibitor.

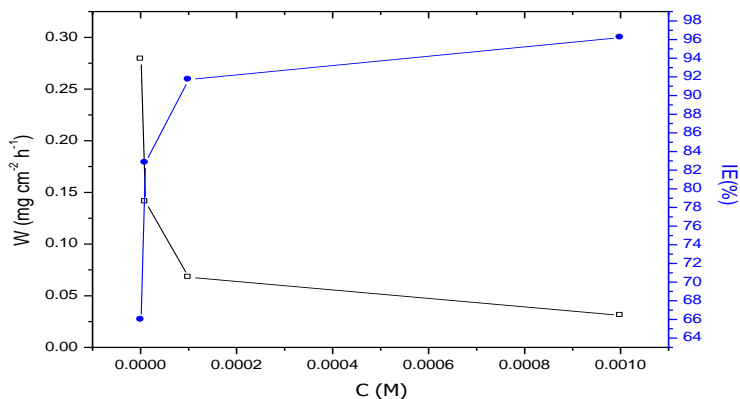


Figure 3: Variation of inhibition efficiency and corrosion rate in 1M HCl on mild steel surface without and with different concentrations of benzothiazine derivatives (P_1).

The adsorption isotherm helps us to provide the information on the interaction between the inhibitor molecule of P_1 and the metal surface. The degree of surface coverage (θ) for different concentrations of inhibitor was evaluated from Weight loss measurements. Attempts were made to fit θ values to various isotherms such as Temkin, Frumkin and Langmuir. The best fit was obtained with the Langmuir isotherm (Figure. 4). From this isotherm θ is linked to concentration inhibitor follow equation (5) [22].

$$\frac{\theta}{1-\theta} = C_{inh} \cdot K_{ads} \quad (5)$$

By rearranging this equation (6):

$$\frac{C_{inh}}{\theta} = \frac{1}{K_{ads}} + C_{inh} \quad (6)$$

Where K_{ads} is the adsorption/desorption equilibrium constant, C_{inh} is the corrosion inhibitor concentration in the solution.

It was found that from Figure 4 (plot of C/θ versus C) gives straight line with slope near to 1, indicating that the adsorption of compound under consideration on mild steel / acidic solution interface obeys Langmuir adsorption. The thermodynamic parameters for the corrosion of mild steel in 1M HCl acid in the presence and absence of different concentrations of benzothiazine derivatives (P_1) is given in the Table 4.

Table 4: Thermodynamic parameters for the corrosion of mild steel in 1 M HCl in the absence and presence of different concentrations of benzothiazine derivatives P_1 .

Inhibitor	Linear correlation (coefficient R)	Slope	K (M^{-1})	ΔG_{ads}° ($kJ \cdot mol^{-1}$)
P_1	0.99999	0.96179	454097.549	-43.62

The free energy of adsorption ΔG_{ads}° can be calculated from the K_{ads} value obtained from the above correlation [23]:

$$\Delta G_{ads}^\circ = -RT \ln (K_{ads} 55.5) \quad (7)$$

Where ΔG_{ads}° is the free energy of adsorption.

Where 55.5 is the concentration of water, $R=8.314J \cdot K^{-1} \cdot mol^{-1}$ is the universal gas constant and T is the absolute temperature (K), K_{ads} the adsorption–desorption equilibrium constant.

The ΔG_{ads}° values are also presented in Table 4, the negative sign of ΔG_{ads}° indicates the spontaneity of the adsorption process and stability of the adsorbed film on the electrode surface [24]. Furthermore, values of ΔG_{ads}° up to $-20 kJmol^{-1}$ are reliable with the electrostatic interaction between the charged molecules and the charged metal (physisorption) while those more negative than $-40 kJmol^{-1}$ involve sharing or transfer of electrons from the inhibitor molecules to the metal surface to form a co-ordinate type of bond (chemisorption) [25]. Accordingly, the value of $\Delta G_{ads}^\circ = -43.62 kJ/mol$ we propose chemisorption of P_1 molecules on the mild steel surface. Infact, because of strong adsorption of H_2O molecules on the surface of steel, it may be assumed that removal of water molecules from the surface is accompanied by chemical interaction between the metal surface and the formed film [23].

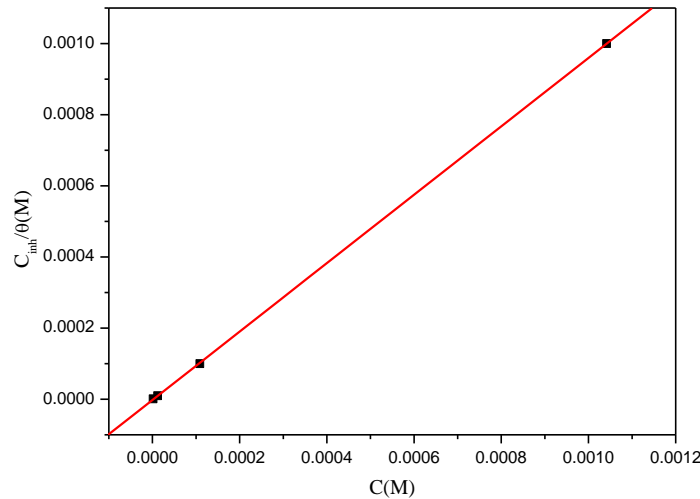


Figure 4: Langmuir adsorption isotherm of P₁ on the steel surface in HCl solution

3.4. Effect of temperature

To investigate the nature of adsorption of the inhibitor and to calculate the activation energies of the corrosion process, weight loss measurements were obtained at different temperatures in the absence and the presence of P₁ and precisely in the range of temperature 313-343K.

Table 5: various corrosion parameters for mild steel in 1M HCl in absence and presence of optimum concentration of benzothiazine derivatives (P₁) at different temperatures.

Temperature (K)	Inhibitor	Corrosion rate (mg/cm ² .h)	θ	IE (%)
313	HCL 1M	1.69	--	--
	P1	0.21	0.88	87.57
323	HCL 1M	3.23	--	--
	P1	0.45	0.86	86.07
333	HCL 1M	6.73	--	--
	P1	1.43	0.79	78.75
343	HCL 1M	10.39	--	--
	P1	2.77	0.73	73.34

Inspection of Table 5 showed that corrosion rate increased with increasing temperature both in uninhibited and inhibited solutions, while the inhibition efficiency of P₁ product decreased with temperature, it might be due to weakening of physical adsorption. In order to calculate activation parameters for the corrosion process, Arrhenius equation (8) and transition state equation (9) were used [26]:

$$C_R = A \exp\left(-\frac{E_a}{RT}\right) \quad (8)$$

$$C_R = \frac{RT}{Nh} \exp\left(\frac{\Delta S_a^\circ}{R}\right) \exp\left(-\frac{\Delta H_a^\circ}{RT}\right) \quad (9)$$

Where E_a is the activation energy of the corrosion process, A is the pre-exponential factor, R the general gas constant, h is the plank's constant, N is Avogadro's number, ΔS_a° is the apparent entropy of activation and ΔH_a° is the apparent enthalpy of activation.

The apparent activation energy (E_a) at optimum concentration of benzothiazine derivatives (P₁) was determined by linear regression between Ln C_R and 1/T (Figure 5) and the results is shown in Table 5. The

linear regression coefficient was close to 1, indicating that the steel corrosion in hydrochloric acid can be elucidated using the kinetic model. Inspection of Table 6 showed that the value of E_a determined in 1M HCl containing our compound is higher ($55.24 \text{ kJ mol}^{-1}$) for benzothiazine derivatives (P_1) than that for uninhibited solution ($79.63 \text{ kJ mol}^{-1}$). The increase in the apparent activation energy may be interpreted as physical adsorption that occurs in the first stage [27]. Szauer and Brand explained that the increase in activation energy can be attributed to an appreciable decrease in the adsorption of the inhibitor on the steel surface with increase in temperature. As adsorption decreases more desorption of inhibitor molecules occurs because these two opposite processes are in equilibrium. Due to more desorption of inhibitor molecules at higher temperatures the greater surface area of steel comes in contact with aggressive environment, resulting increased corrosion rates with increase in temperature [28].

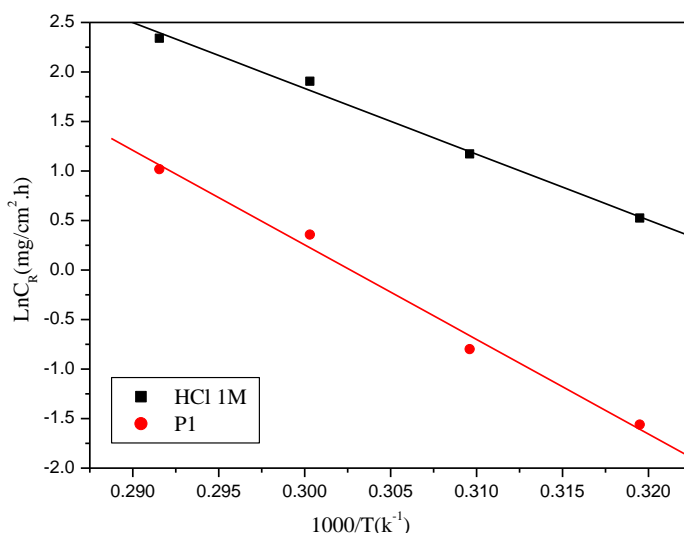


Figure 5: Arrhenius plots of $\text{Ln } C_R$ vs. $1/T$ for steel in 1M HCl in the absence and the presence of benzothiazine derivatives (P_1) at optimum concentration.

Figure 6 showed a plot of $\text{Ln } (C_R/T)$ versus $1/T$. The straight lines are obtained with a slope $(\frac{\Delta H_a^\circ}{RT})$ and an intercept of $(\text{Ln } \frac{RT}{Nh} + \frac{\Delta S_a^\circ}{R})$ from which the values of ΔH_a° and ΔS_a° are calculated and are given in Table 6. Inspection of these data revealed that the thermodynamic ΔH_a° and ΔS_a° parameters for dissolution reaction of steel in 1M HCl in the presence of inhibitor is higher 76.63 and -13.69 kJ/mol than that of in the absence of inhibitor (52.51 and -72.95 kJ/mol respectively). The positive sign of ΔH_a° reflect the endothermic nature of the steel dissolution process suggesting that the dissolution of steel is slow [29] in the presence of inhibitor.

Table 6: Activation parameters for the steel dissolution in 1M HCl in the absence and the presence of benzothiazine derivatives (P_1) at optimum concentration.

Inhibitor	A (Ohm.cm ²)	Linear regression coefficient (r)	E_a (kJ/mol)	ΔH_a° (kJ mol ⁻¹)	ΔS_a° (kJ mol ⁻¹)
HCl 1M	1.49 10⁶	0.99742	55.24	52.51	-72.95
P_1	2.21 10⁶	0.99663	79.63	76.63	-13.69

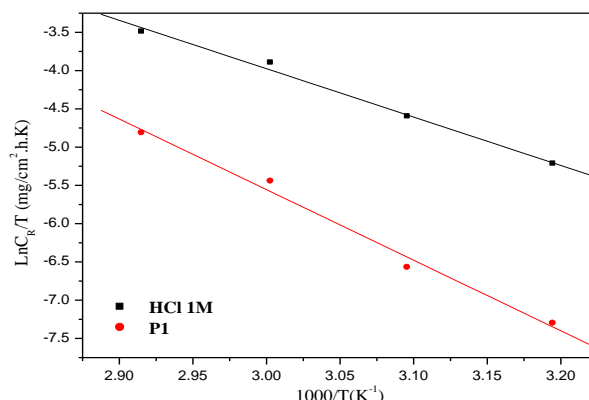


Figure 6: Arrhenius plots of $\ln(C_R/T)$ vs. $1/T$ for steel in 1M HCl in the absence and the presence of benzothiazine derivatives (P_1) at optimum concentration.

The large negative value of mild steel in 1M HCl implies that the activated complex is the rate-determining step, rather than the dissociation step. In the presence of the inhibitor, the value of ΔS_a° increases and is generally interpreted as an increase in disorder as the reactants are converted to ΔS_a° the activated complexes [30]. The values of ΔS_a° reflect the fact that the adsorption process is accompanied by an increase in entropy, which is the driving force for the adsorption of the inhibitor onto the steel surface.

4. COMPUTATIONAL DETAILS

All quantum chemical study was carried out using the Density Functional Theory (DFT) with hybrid functional B3LYP, based on Becke's three-parameter functional including Hartree-Fock exchange contribution with a nonlocal correction for the exchange potential proposed by Becke [31,32] together with the nonlocal correction for the correlation energy provided by Lee and al.[33].

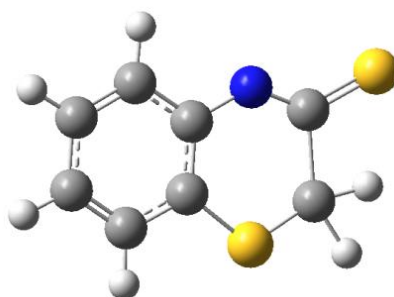


Figure 7: Optimized structures of benzothiazine derivatives (P_1)

Parameters obtained from the quantum chemical calculations including the energy of highest occupied molecular orbital (E_{HOMO}), the energy of lowest unoccupied molecular orbital (E_{LUMO}), the separation energy ($\Delta E = E_{LUMO} - E_{HOMO}$) and the dipole moment (μ) are shown in Table 7.

In terms of the frontier molecular orbital theory, HOMO and LUMO energies may be used to predict the adsorption centers of the inhibitor molecules responsible for the interaction with surface metal atoms. As E_{HOMO} is often associated with the electron donating ability of the molecule, high values of E_{HOMO} mean that the molecule is tended to donate electrons to appropriate acceptor molecules with low energy and empty molecular orbital. Conversely, lower E_{LUMO} values indicate the stronger ability of the molecule to accept electrons. Therefore, the ΔE value represents an important stability index that helps to predict the inhibitive effect of the calculated molecules [34, 35]. The other important parameter is dipole moment, which can lead to increase of inhibition and can be related to the dipole-dipole interaction of molecules and metal surface [36, 37].

As we know, frontier orbital theory is useful in predicting the adsorption centers of the inhibitors responsible for the interaction with surface metal atoms. figure 8, show the HOMO and LUMO orbital contributions for

the studied inhibitor molecule benzothiazine. For the molecule, the HOMO and LUMO densities were concentrated on rings, N atom and S-atom. This means that these are active sites of the molecules responsible for interaction with metal surface.

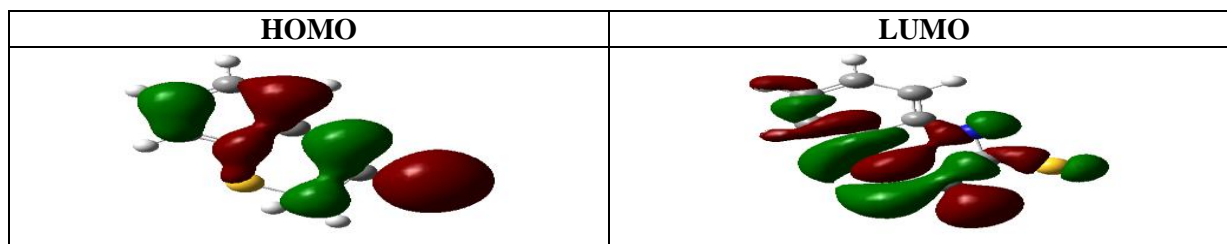


Figure 8: the frontier molecular orbital density distribution of benzothiazine derivatives (P_1).

Table 7 : Calculated quantum chemical parameters of the studied benzothiazine derivatives (P_1).

Quantum parameters	P_1
E_{HOMO} (u.a.)	-0.18846
E_{LUMO} (u.a.)	-0.13113
ΔE_{gap} (u.a.)	0.05733
μ (debye)	7.1376

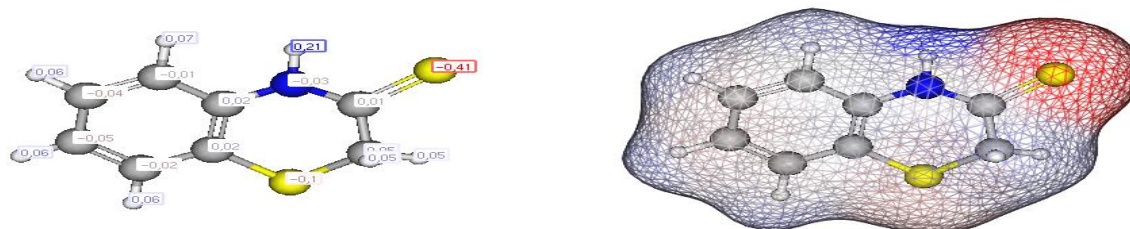


Figure 9: Charge repartition of benzothiazine derivatives (P_1)

It has been reported that the more negative the atomic charge of the adsorbed centre, the more easily the atom donates its electrons to the unoccupied orbital of metal [38-40]. Figure 9 shows the Mulliken charges of the atoms in benzothiazine molecule. By careful inspection of the values of Mulliken charges, the largest negative atom is found on the N (-0.03) of the benzothiazine thione ring. Other atoms with excess negative charges include S of thione group. This is further supported by figure 9, where the total electron density is located around these atoms.

Conclusion

3, 4-dihydro-2H-1,4-benzothiazine-3-thione P_1 was found to be an inhibitor for the corrosion of mild steel in HCl solution. Inhibition efficiency increases with increase in benzothiazine derivatives (P_1) concentration, but decrease with increase in temperature. Double-layer capacitances decrease with respect to blank solution when the synthesized inhibitor is added. This fact can be explained by adsorption of the synthesized inhibitor species on the steel surface. Polarization studies reveal that P_1 act as a mixed-type inhibitor. The adsorption of P_1 on mild steel surface can be approximated by Langmuir isotherm model. The smaller gap between E_{HOMO} and E_{LUMO} favors the adsorption of the synthesized inhibitor on steel surface and enhancement of corrosion inhibition.

References

- Rathore B.S., Kumar M., *Bioorg. Med. Chem.* 14 (2006) 5678.
- Barazarte A., Camacho J., Dominguez J., Lobo G., Gamboa N., Rodrigues J., Capparelli M.V., Alvarez-Larena A., Andujar S., Enriz D., Charris J., *Bioorg. Med. Chem.* 16 (2008) 3661.
- Chia E.W., Pearce A.N., Berridge M.V., Larsen L., Perry N.B., Sansom C.E., Godfrey C.A., Hanton L.R., Guo-Liang Lu, Walton M., Denny W.A., Webb V.L., Copp B.R., Harper J.L., *Bioorg. Med. Chem.* 16 (2008) 9432.
- Fringuelli R., Schiaffella F., Bistoni F., Pitzurra L., Vecchiarelli A., *Bioorg. Med. Chem.* 6 (1998) 103.

5. Bakavoli M., Nikpour M., Rahimizadeh M., Saberi M.R., Sadeghian H., *Bioorg. Med. Chem.* 15 (2007) 2120.
6. Zarrok H., Al-Deyab S. S., Zarrouk A., Salghi R., Hammouti B., Oudda H., Bouachrine M., Bentiss F., *Int. J. Electrochem. Sci.* 7 (2012) 4047.
7. Zarrok H., Salghi R., Zarrouk A., Hammouti B., Oudda H., Bazzi Lh., Bammou L., Al-Deyab S. S., *Der. Pharm. Chem.* 4 (2012) 407.
8. Harmaoui A., El Fal M., Boudalia M., Tabyaoui M., Guenbour A., Bellaouchou A., Ramli Y., Essassi E.M., *J. Mater. Environ. Sci.* 6 (2015) 2509.
9. Ghazoui A., Saddik R., Benchat N., Hammouti B., Guenbour M., Zarrouk A., Ramdani M., *Der. Pharm. Chem.* 4 (2012) 352.
10. Chetouani A., Hammouti B., Benhadda T., Daoudi M., *Appl. Surf. Sci.* 249 (2005) 375.
11. Mu G., Li X., Qu Q., Zhou J., *Corros. Sci.* 48 (2006) 445.
12. Umoren S.A., Obot I.B., Ebenso E.E., Okafor P. C., Ogbobe O., Oguzi E. E., *Anti. Corros. Meth. Mater.* 53 (2006) 277.
13. Bockris J.O.M, Drazic D., *Electrochem. Acta.* 7(1962) 293
14. suru T., Haruyama T., Gijutsu S., *Jpn. B.J. Soc. Corros. Eng.* 27 (1978) 573.
15. Aljourani J., Raeissi K., Golozar M.A., *Corros. Sci.* 51 (2009) 1836.
16. Boudalia M., Bellaouchou A., Guenbour A., Bourazmi H., Tabyaoui M., El Fal M., Ramli Y., Essassi E.M., Elmsellem H., *Mor. J. Chem.* 2 (2014) 97.
17. Aljourani J., Raeissi K., Golozar M. A., *Corros. Sci.* 51 (2009) 1836.
18. Every R.L., Riggs O.L., *Mat. Prot.* 3 (1964) 46.
19. El-Awady A. A., Abd-El-Nabey B A., Aziz S .G., *J. Electrochem. Soc.* 139 (1992) 2149.
20. Bockris J.O.M., Reddy A.K.N., *Modern Electrochemistry, Plenum Pub. Corp. New York.* 2 (1976).
21. Wang X., Yang H., Wang F., *Corros. Sci.* 52 (2010) 1268.
22. Sanat kumar B. S., Nayak J., Shetty A.N., *Coat. J. Technol. Res.* 4 (2011) 1.
23. AliAnejjar A., Salghi R., Zarrouk A., Zarrok H., Benali O., Hammouti B., Al-Deyab S.S., Benchat N-E., Saddik R., DOI10.1007/s11164-013-1244-7, *Res. Chem. Intermed.* 41 (2015) 913.
24. Hussin M. H., Kassim M., *J. Mater. Chem. Phys.* 125 (2011) 461.
25. Benali O., Larabi L., Traisnel M., Gengenbre L., Harek Y., *Surf. Sci.* 253 (2007) 6130.
26. Lodha S. R., *Pharmaceut Res.* 6(2008)1.
27. Bockris J.O., Reddy A.K.N., *Modern Electrochemistry, Plenum Press, New York,* 2 (1977) 1267.
28. Szauer T., Brand A., *Electrochim. Acta.* 26 (1981) 1219.
29. Lotfi N., Lgaz H., Belkhaouda M., Larouj M., Salghi R., Jodeh S., Oudda H., Hammouti B., *Ar. J. Chem. Environ. Res.* 1(1) (2014) 13-23
30. El Ouali I., Hammouti B., Aouniti A., Ramli Y., Azougagh M., Essassi E.M., Bouachrine M., *J.Mater. Environ. Sci.* 1 (2010) 1.
31. Becke A.D., *Chem. Phys.* 98 (1993) 5648.
32. Becke A.D., *Phys. Rev. A.* 38 (1988) 3098.
33. Lee C., Yang W., Parr R.G., *Phys. Rev. B.* 37 (1988) 785.
34. Bereket G., Ogretir C., Hur E.J., *J. Mol. Struct.* 578 (2002) 79.
35. Qiong Deng, Hong-Wei Shi, Na-Na Ding, Bao-Qin Chen, Xiao-Peng He, Guixia Liu, Yun Tang, Yi-Tao Long, Guo-Rong Chen., *Corros. Sci.* 57 (2012) 220.
36. Dogru Mert, B., Mert, M.E., Kardas, G., *Corros. Sci.* 53 (2011) 4265.
37. Ayse Ongun Yuce, Basak Dogru Mert, Gulfeza Kardas, Birgul Yazıcı. *Corros. Sci.* 83 (2014) 310.
38. Obot I.B., Obi-Egbedi N.O., *Mater. Chem. Phys.* 122(2-3)(2010)325.
39. Elmsellem H., Aouniti A., Youssoufi M.H., Bendaha H., Ben hadda T., Chetouani A., Warad I., Hammouti B., *Phys. Chem. News.* 70 (2013) 84.
40. Elmsellem H., Elyoussfi A., Sebbar N.K., Dafali A., Cherrak K., Steli H., Essassi E.M., Aouniti A., Hammouti B., *Maghreb. J. Pure & Appl. Sci.*, 1 (2015) 1-10

(2015); <http://www.jmaterenvirosci.com>